

# NJC

Accepted Manuscript



This is an *Accepted Manuscript*, which has been through the Royal Society of Chemistry peer review process and has been accepted for publication.

*Accepted Manuscripts* are published online shortly after acceptance, before technical editing, formatting and proof reading. Using this free service, authors can make their results available to the community, in citable form, before we publish the edited article. We will replace this *Accepted Manuscript* with the edited and formatted *Advance Article* as soon as it is available.

You can find more information about *Accepted Manuscripts* in the [Information for Authors](#).

Please note that technical editing may introduce minor changes to the text and/or graphics, which may alter content. The journal's standard [Terms & Conditions](#) and the [Ethical guidelines](#) still apply. In no event shall the Royal Society of Chemistry be held responsible for any errors or omissions in this *Accepted Manuscript* or any consequences arising from the use of any information it contains.

## ARTICLE

Cite this: DOI: 10.1039/x0xx00000x

Received 00th January 2012,  
Accepted 00th January 2012

DOI: 10.1039/x0xx00000x

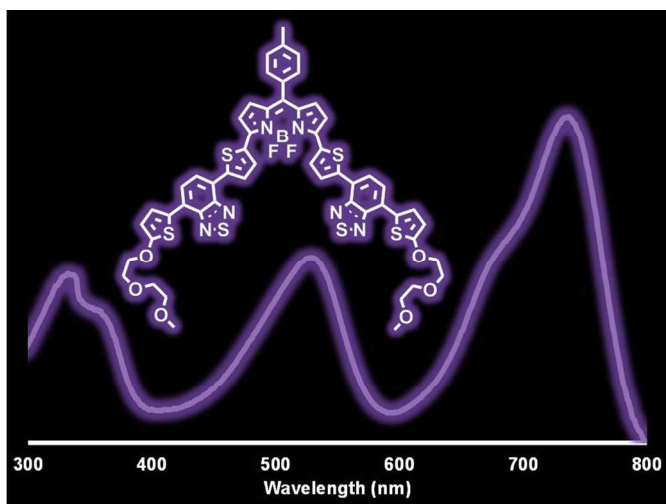
www.rsc.org/

## Deep-purple-grey Thiophene-benzothiadiazole-thiophene BODIPY Dye for Solution-processed Solar Cells

Antoine Mirloup,<sup>a</sup> Nicolas Leclerc,<sup>b</sup> Sandra Rihn,<sup>a</sup> Thomas Bura,<sup>a</sup> Rony Bechara,<sup>c</sup> Anne Hébraud,<sup>b</sup> Patrick Lévêque,<sup>c</sup> Thomas Heiser,<sup>c</sup> Raymond Ziessel<sup>\*a</sup>

### Graphical Abstract

Original flat thiophene-benzothiadiazole-thiophene BODIPY dyes have been engineered without unsaturated linkers for solution processed solar cells.



## ARTICLE

# Deep-purple-grey Thiophene-benzothiadiazole-thiophene BODIPY Dye for Solution-processed Solar Cells

Cite this: DOI: 10.1039/x0xx00000x

Received 00th January 2012,  
Accepted 00th January 2012

DOI: 10.1039/x0xx00000x

www.rsc.org/

Antoine Mirloup,<sup>a</sup> Nicolas Leclerc,<sup>b</sup> Sandra Rihn,<sup>a</sup> Thomas Bura,<sup>a</sup> Rony Bechara,<sup>c</sup> Anne Hébraud,<sup>b</sup> Patrick Lévêque,<sup>c</sup> Thomas Heiser,<sup>c</sup> Raymond Ziessel<sup>\*a</sup>

In this work we explore the synthesis of extended 4,4-difluoro-4-bora-3a,4a-diaza-s-indacene dye (BODIPY) engineered from thiophene-benzothiadiazole-thiophene modules linked in the 3,5-substitution positions. We found that this highly soluble dye absorbs until 800 nm in solution and up to 900 nm in thin films. An effective charge transfer absorption band was found around 479 nm. The hybrid dye emits at 778 nm with a quantum yield of about 6%. Similar electrochemical and optical gaps were determined about 1.36 eV. When deposited in thin films the dye exhibit an ambipolar nature with well-balanced hole and electron mobilities. Bulk heterojunction solar cells based upon this dye blended with [6,6]phenylC<sub>61</sub>or<sub>71</sub>butyric acid methylester (PC<sub>61</sub>BM or PC<sub>71</sub>BM) provide a power conversion efficiency of about 1.26% after a mild thermal annealing.

## 1. Introduction

The engineering of photoactive dyes for application in organic (opto)-electronics and photovoltaic devices is a multi-parameter challenge. The most innovative materials involve both the optimization of the functional units responsible for the colour and for the hole transport and the optimization of its combination with electron acceptor moiety in a molecular (or supramolecular) bulk heterojunction (BHJ) suitable for the targeted application.<sup>1,2</sup> Because of significant issues related to the availability of innovative dyes, the photostability, the charge carrier mobility, the light harvesting properties, boron dipyrromethene dyes (BODIPY's) are generally regarded as highly promising and loosely studied candidates for photovoltaic applications.<sup>3</sup> Very recently, we became interested in the construction of BODIPY dyes containing bis-thiophene heterocyclic ring system linked in the 3,5-substitution positions via unsaturated linkers. These green absorbing dyes ( $\lambda_{\text{abs}} > 700$  nm) display attractive optical and interesting charge transporting properties and were highly efficient when blended with PC<sub>61</sub>BM (electron acceptor) in bulk heterojunction (BHJ) solar cells.<sup>4</sup> Our interest in this specific design relies on the fact that large-scale synthesis of purified compounds could be achieved in a minimum of synthetic steps.

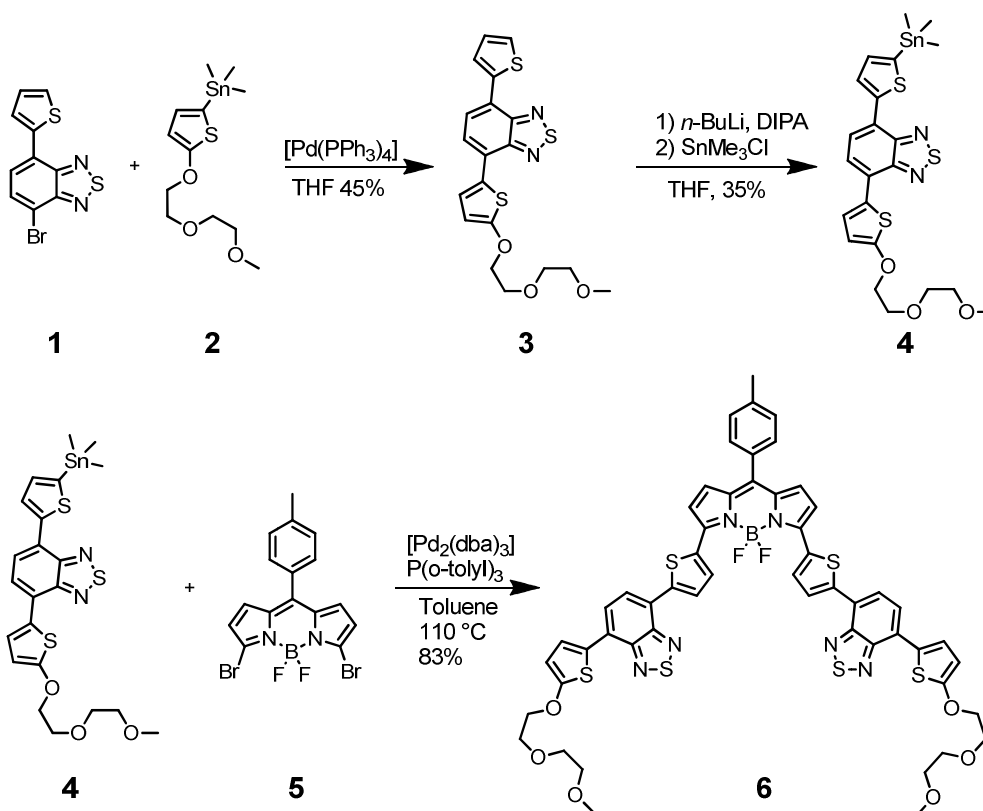
In the course of such work it appears important to decipher the key elements to understand the system, find new synthetic

options for the design of even more efficient and sustainable materials. Along this line of using small-molecules as organic donors several types of dyes have been scrutinized and classified as oligothiophenes,<sup>5</sup> diketopyrrolopyrrole (DPP),<sup>6</sup> squaraine,<sup>7</sup> hexabenzocoronenes,<sup>8</sup> merocyanine,<sup>9</sup> donor-acceptor oxindane,<sup>10</sup> and thiadiazolo-bithienyl dyes.<sup>11</sup> Boron dipyrromethene (BODIPY) dyes<sup>3,12</sup> are characterized by outstanding chemical and photochemical stabilities, redox activity and optical features that can easily be tailored by chemical transformation, allowing them to be used in BHJ solar cells,<sup>13,14</sup> and dye sensitized solar cells.<sup>15,16,17</sup>

A logical progression in the design of novel dyes usable in BHJ solar cells is to use the molecular items present in low-band-gap polymers systems such as thieno[3,2-*b*]thiophene,<sup>18</sup> N-alkyldithienopyrrole,<sup>19</sup> thiazolothiazole-thiophene,<sup>20</sup> dithienosilole,<sup>21</sup> benzodithiophene,<sup>22</sup> benzothiadiazole,<sup>23</sup> bithiopheneimide.<sup>24</sup> Not only should this unit contribute in the hole transporting properties, but it should also guarantee the ability of highly coloured materials when linked in the 3,5-positions of the BODIPY.

We have now designed dye **6** (Scheme 1) based on bithiophene-benzothiadiazole modules according to the push-pull-push BODIPY format associated to the building of highly coloured dyes. This design principle popularized earlier, is attractive due to its modular nature. In the present design the hole transporting subunits were directly attached to the

BODIPY core avoiding unsaturated (alkyne or vinyl) linkers. The novel dye **6** was prepared according to Scheme 1.



**Scheme 1.** General synthetic sketch for the preparation of dye **6**.

## 2. Experimental Part

### 2.1. General methods

All reactions were performed under an atmosphere of dried argon using standard Schlenk tube techniques. All chemicals were used as received from commercial sources unless stated otherwise. THF was distilled from sodium and benzophenone under an Ar atmosphere.  $^1\text{H}$  NMR (400.1 MHz) and  $^{13}\text{C}$  NMR (100.5 MHz) spectra were recorded at room temperature (rt) on a Bruker Advance 400 MHz spectrometer,  $^1\text{H}$  NMR (300.1 MHz) and  $^{13}\text{C}$  NMR (75.5 MHz) or a Bruker Advance 300 MHz spectrometer,  $^1\text{H}$  NMR (200.1 MHz) and  $^{13}\text{C}$  NMR (50.5 MHz) or a Bruker Advance 200 MHz spectrometer using perdeuterated solvents as internal standards. Chromatographic purifications were performed using silica gel (40–63  $\mu\text{m}$ ). TLC was performed on silica gel plates coated with fluorescent indicator.

Absorption spectra were recorded on a Shimadzu UV-3000 absorption spectrometer. The steady-state fluorescence emission and excitation spectra were obtained by using a HORIBA JOBIN YVON FLUOROMAX 4. All fluorescence spectra were corrected. The fluorescence quantum yield ( $\Phi_{\text{exp}}$ ) was calculated from eq 1.

$$(1) \quad \Phi_{\text{exp}} = \Phi_{\text{Ref}} \frac{I}{I_{\text{Ref}}} \frac{OD_{\text{Ref}}}{OD} \frac{\eta^2}{\eta_{\text{Ref}}^2}$$

Here,  $I$  denotes the integral of the corrected emission spectrum,  $OD$  is the optical density at the excitation wavelength and  $\eta$  is the refractive index of the medium. The reference systems used were rhodamine 6G ( $\Phi = 0.78$ ) in air equilibrated water and Tetramethoxydiisoindomethene-difluoroborate ( $\Phi = 0.51$ ). Luminescence lifetimes were measured on an Edinburgh Instruments spectrofluorimeter equipped with a R928 photomultiplier and a PicoQuant PDL 800-D pulsed diode connected to a GwInstect GFG- 8015G delay generator. No filter was used for the excitation. Emission wavelengths were selected by a monochromator. Lifetimes were deconvoluted with FS-900 software using a light-scattering solution (LUDOX) for instrument response.

Potentials were determined by cyclic voltammetry in deoxygenated  $\text{CH}_2\text{Cl}_2$  solutions, containing 0.1 M TBAPF<sub>6</sub>, at a solute concentration range of ca 1 mM and at rt. Potentials are given versus the saturated calomel electrode (SCE) and standardized vs ferrocene (Fc) as internal reference assuming that  $E_{1/2}(\text{Fc}/\text{Fc}^+) = +0.38 \text{ V}$  ( $\Delta E_p = 60 \text{ mV}$ ) vs SCE. The error in half-wave potential is  $\pm 10 \text{ mV}$ . Where the redox processes are irreversible, the peak potentials ( $E_{\text{ap}}$  or  $E_{\text{cp}}$ ) are quoted. All reversible redox steps result from one-electron processes unless otherwise specified.

### 2.2. Preparative work

**Materials.** Compounds **1**<sup>23</sup>, **2**<sup>4</sup> and **5**<sup>24</sup> were synthesized according to the indicated literature procedure.

**Compound 3.** Compound **1** (0.9 g, 3.03 mmol), compound **2** (3.3 g, 12.8 mmol) and THF (25 mL) were placed in a 100 mL flask. The solution was degazed with argon for 20 minutes and then [Pd(PPh<sub>3</sub>)<sub>4</sub>] (0.35 g, 0.3 mmol) was added. The solution was stirred and heated to reflux for one day. After cooling down, the mixture was washed with water and extracted with ethyl acetate. Organic extracts were dried over anhydrous magnesium sulfate or absorbent cotton, and the solvent was removed on a rotator evaporator. The crude product was purified by column chromatography (silica gel, solvent: 80/20 cyclohexane/AcOEt). The product was then recrystallized in acetone to obtain a red powder (570 mg, 43%). <sup>1</sup>H NMR (acetone d<sub>6</sub>, 300 MHz): δ 3.32 (s, 3H), 3.54 (t, <sup>3</sup>J = 5.2 Hz, 2H), 3.68 (t, <sup>3</sup>J = 5.2 Hz, 2H), 3.87 (t, <sup>3</sup>J = 4.6 Hz, 2H), 4.34 (t, <sup>3</sup>J = 4.6 Hz, 2H), 6.46 (d, <sup>3</sup>J = 4.2 Hz, 1H), 7.25 (dd, <sup>3</sup>J = 5.1 Hz, <sup>4</sup>J = 1.0 Hz, 1H), 7.84 (d, <sup>3</sup>J = 7.7 Hz, 1H), 7.82 (d, <sup>3</sup>J = 4.2 Hz, 1H), 7.99 (d, <sup>3</sup>J = 7.7 Hz, 1H), 8.17 (dd, <sup>3</sup>J = 3.7 Hz, <sup>4</sup>J = 1.0 Hz, 1H). <sup>13</sup>C NMR (acetone d<sub>6</sub>, 75 MHz): δ 59.6, 70.7, 72.0, 73.4, 74.7, 105.5, 125.3, 126.1, 126.9, 127.5, 127.7, 128.0, 128.5, 128.8, 129.4, 140.8, 153.8, 154.0, 168.9. EIMS, m/z (%): 418.0 ([M], 100). Anal. Calcd for C<sub>19</sub>H<sub>18</sub>N<sub>2</sub>O<sub>3</sub>S<sub>3</sub> (Mr = 418.55): C, 54.52; H, 4.33; N, 6.69; Found: C, 54.33; H, 4.47; N, 6.42.

**Compound 4.** 0.426 mL of a solution of *n*-BuLi at 2.5 M in hexane were added dropwise in a solution of diisopropylamine (0.164 mL, 1.17 mmol) in 10 mL of distilled THF at -78 °C. The solution was warmed up to -40 °C for 30 min and then was cooled again at -78 °C. A solution of compound **3** (0.41 g, 0.97 mmol) in 5 mL of THF was then added at -78 °C. The mixture was stirred at room temperature for 12 h. The reaction was quenched with a saturated solution of NH<sub>4</sub>Cl. The mixture was washed with water and extracted with ethyl acetate. Organic extracts were dried over anhydrous magnesium sulfate or absorbent cotton, and the solvent was removed on a rotator evaporator. No further purification is possible for this stanic compound and the conversion yield was estimated by <sup>1</sup>H NMR around 35%. <sup>1</sup>H NMR (CDCl<sub>3</sub>, 300 MHz): δ 0.44 (s, 9H), 3.41 (s, 3H), 3.61 (t, <sup>3</sup>J = 4.9 Hz, 2H), 3.74 (t, <sup>3</sup>J = 4.5 Hz, 2H), 3.89 (t, <sup>3</sup>J = 4.9 Hz, 2H), 4.31 (t, <sup>3</sup>J = 4.6 Hz, 2H), 6.33 (d, <sup>3</sup>J = 4.2 Hz, 2H), 7.28 (d, <sup>3</sup>J = 3.5 Hz, 1H), 7.63 (d, <sup>3</sup>J = 7.6 Hz, 1H), 7.81 (m, 2H), 8.14 (d, <sup>3</sup>J = 3.5 Hz, 1H).

**Compound 6.** Compound **4** (160 mg, 0.275 mmol), compound **5** (48 mg, 0.110 mmol), distilled toluene (10 mL) and tri(*o*-tolyl)phosphine (7 mg, 21 μmol) were added in a Schlenk tube. The solution was degazed with argon for 45 min. [Pd<sub>2</sub>(dba)<sub>3</sub>] (5 mg, 5.5 μmol) was then added and the mixture was heated at 110 °C for 3 h. After cooling down, the mixture was washed with water and extracted with dichloromethane. Organic extracts were dried over anhydrous magnesium sulfate or absorbent cotton, and the solvent was removed on a rotator evaporator. The crude product was purified by column chromatography (silica gel, solvent: 90/10 dichloromethane/ethyl acetate). The obtained product was then recrystallised in dichloromethane/pentan to obtain a purple

powder (102 mg, 83%). <sup>1</sup>H NMR (CDCl<sub>3</sub>, 400 MHz): δ 2.48 (s, 3H), 3.41 (s, 6H), 3.59-3.61 (m, 4H), 3.73-3.75 (m, 4H), 3.89-3.91 (m, 4H), 4.30-4.32 (m, 4H), 6.34 (d, <sup>3</sup>J = 4.1 Hz, 2H), 6.82 (d, <sup>3</sup>J = 4.2 Hz, 2H), 6.95 (d, <sup>3</sup>J = 4.3 Hz, 2H), 7.32 (d, <sup>3</sup>J = 7.7 Hz, 2H), 7.43 (d, <sup>3</sup>J = 7.8 Hz, 2H), 7.63 (d, <sup>3</sup>J = 7.5 Hz, 2H), 7.83 (d, <sup>3</sup>J = 4.0 Hz, 2H), 7.87 (d, <sup>3</sup>J = 7.9 Hz, 2H), 8.13 (d, <sup>3</sup>J = 4.1 Hz, 2H), 8.38 (d, <sup>3</sup>J = 4.2 Hz, 2H). <sup>13</sup>C NMR (CDCl<sub>3</sub>, 75 MHz): δ 21.6, 29.8, 59.3, 69.6, 71.0, 72.1, 73.2, 106.7, 121.0, 123.9, 124.2, 126.1, 126.4, 126.8, 127.2, 129.2, 130.0, 130.8, 131.9, 135.5, 140.4, 152.6, 152.8, 167.3. EIMS, m/z (%): 1114.1 ([M], 100). Anal. Calcd for C<sub>54</sub>H<sub>45</sub>BF<sub>2</sub>N<sub>6</sub>O<sub>6</sub>S<sub>6</sub> (Mr = 1115.17): C, 58.16; H, 4.07; N, 7.54; Found: C, 57.94; H, 3.82; N, 7.38.

### 2.3. Device preparation

Bulk heterojunction devices were elaborated using dye **6** as electron donor and PC<sub>61</sub>BM or PC<sub>71</sub>BM as electron acceptor. Chloroform and chlorobenzene (CB) were used as solvents with typical dye **6** concentrations ranging from 3 to 10 mg/mL. For all CB mixtures, DIO with volumic concentration ranging from 0.3 to 0.5 % were tested. The standard device structure was the following: ITO/PEDOT:PSS (~40 nm)/active layer/Al (~120 nm). For the most promising results, the cathode was replaced by a Ca(20 nm)/Al(120 nm) bilayer. Indium Tin Oxide coated glass with a surface resistance lower than 20 Ω/sq was used as transparent substrate. Substrates were cleaned sequentially by ultrasonic treatments in acetone, isopropyl alcohol, and deionized water. After an additional cleaning for 30 minutes under ultra-violet generated ozone, a highly conductive polyethylene dioxythiophene: polystyrene-sulphonate PEDOT:PSS was spin coated (1500 rpm: 40 nm) from an aqueous solution and dried for 30 minutes at 120 °C under vacuum before being transferred to the nitrogen filled glove box. The chloroform or chlorobenzene molecule/PCBM solutions were stirred for at least 24 hours at 50 °C before spin-coating. The relative dye **6**/PCBM weight ratio was varied from 1/1 to 1/2. The active layer spin coating conditions (one fast and one slow program) were also varied to change the active layer thickness. Both spin coating programs included two steps with the following parameters: step 1 (2000 rpm, 120 seconds and 600 rpm/s) and step 2 (2500 rpm, 60 seconds and 600 rpm/s) for the “fast” program and step 1 (1200 rpm, 60 seconds and 200 rpm/s) and step 2 (2000 rpm, 120 seconds and 200 rpm/s) for the “slow” one. Finally, a 120 nm thick aluminum layer with or without a pre-20 nm thick calcium layer was thermally evaporated and used as cathode. The device active area was 12 mm<sup>2</sup>, while each sample included four independent diodes. Current versus Voltage (J-V) characteristics were measured using a source measurement unit Keithley 2400 under darkness and under AM1.5G (100 mW/cm<sup>2</sup>) illumination. The standard illumination was provided by Sun 3000 (ABET Technologies) solar simulator and the illumination power was set using a calibrated silicon solar cell. The photovoltaic cells elaboration after substrate preparation and the characterizations were performed in nitrogen ambient.

### 3. Results and discussion

#### 3.1. Synthesis and characterisation

Molecules **1**,<sup>25</sup> **2**<sup>4</sup> and **5**<sup>26</sup> were prepared according to procedures found in literature. The first step consists of a Stille coupling reaction between **1** and **2**. This reaction is carried out under standard conditions using palladium(0) catalysts and leads to trimer **3** with 43% yield. In a second step the stannic group is introduced by the formation of the lithiated thiophene in the last free  $\alpha$ -position of thiophenes thanks to LDA, which then reacts with trimethyltin chloride leading to compound **4**. The obtained crude product is not purified, as stannic compounds are not quite stable on silica gel, and the conversion is estimated by <sup>1</sup>H NMR spectroscopy (around 35%). The resulting mixture is then engaged in another Stille coupling reaction with the dibromo-BODIPY **5**. The fraction of **3** that did not react to form the stannic compound **4** is recovered and can be recycled. The target compound **6** is obtained in 83 % yield. The proton NMR is a diagnostic for the desired molecule. In particular, the proton NMR spectra displays ten proton patterns in the aromatic window as would be expected from a first order spectrum and proves that the molecule has a symmetry axis bisecting the tolyl and the BF<sub>2</sub> fragments. The short polyoxoethylene chains also display four characteristic patterns in the 3.5 to 4.5 ppm range. All other routine analysis (<sup>13</sup>C, EI-MS and elemental analysis) are in keeping with the molecular assignment.

The rationale to use polyoxoethylene short chains is based on previous observations: i) highly pure material could be prepared due to polarity imported by the oxygen atoms; ii) high solubility in most common solvents and iii) good filmability and increase of dye stability.

#### 3.2. Spectroscopic characterization

The absorption, emission and excitation spectra of the trimer thiophene-benzothiadiazole-thiophene (T-Bz-T) **3** and the final compound **6** are shown in Figures 1 and 2. The absorption spectrum of **3** shows two intense peaks. The first absorption around 320 nm corresponds to a  $\pi$ - $\pi^*$  transition with an extinction coefficient  $\epsilon$  about 28,000 M<sup>-1</sup>cm<sup>-1</sup>. The second absorption peak, around 479 nm is broader and is likely a charge transfer band (CT) due to the presence of a strong donor (the thiophene subunit) and a strong acceptor (the benzothiadiazole moiety) in the trimer. The  $\epsilon$  value of the CT band is weaker than the  $\pi$ - $\pi^*$  transition one by about 15,000 M<sup>-1</sup>cm<sup>-1</sup>. Excitation at 450 nm gave the emission spectrum with a maximum at 631 nm, this emission being independent of excitation wavelength (Figure 1). The excitation spectrum matches the absorption spectrum, a result excluding aggregation or the presence of impurities. The large Stokes shift (about 5,000 cm<sup>-1</sup>) and a long lifetime (about 10 ns) confirm the CT nature of this transition. However, there was no influence of the solvent (THF, dichloromethane, toluene) on the spectroscopic characteristics of **3** and its quantum yield was around 62 %. The radiative rate constant is larger than the non-radiative rate constant confirming the efficiency of the process (Table 1).

**Table 1.** Spectroscopic data for **3** and **6** in THF.

Compd.	$\lambda_{\text{abs}}$ (nm)	$\epsilon$ (M <sup>-1</sup> .cm <sup>-1</sup> )	$\lambda_{\text{em}}$ (nm)	$\Phi_F$ ( $\lambda_{\text{ex}}$ , nm)	$\tau$ (ns)	$k_r^{\text{a}}$ (10 <sup>7</sup> s <sup>-1</sup> )	$k_{\text{nr}}^{\text{b}}$ (10 <sup>7</sup> s <sup>-1</sup> )	$\Delta_{\text{ss}}^{\text{c}}$ (cm <sup>-1</sup> )	FWHM <sup>d</sup> (cm <sup>-1</sup> )
<b>3</b>	320 (479 for CT band)	15,500	631	0.62 (@450)	10.5	5.90	3.62	5030	4200
<b>6</b>	737	93,800	778	0.06 (@680) <sup>e</sup>	1.3	4.55	71.8	720	1900

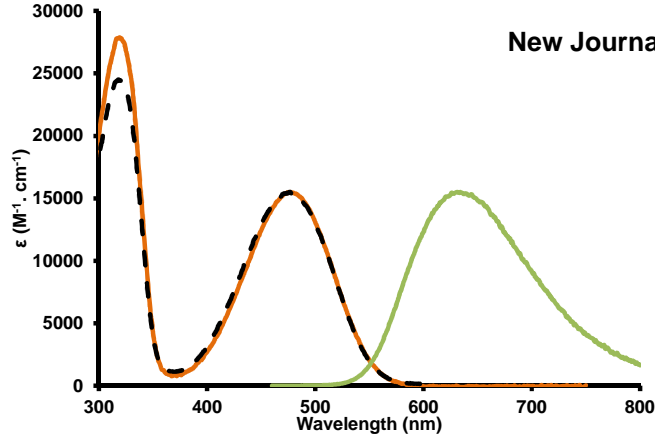
a)  $k_r$  was calculated from  $\Phi_F = \frac{k_r}{k_r + k_{\text{nr}}} = k_r \tau$ .

c)  $k_{\text{nr}}$  was calculated from  $k_{\text{nr}} = \frac{1 - \Phi_F}{k_r}$ .

c) Stoke shifts

d) Full width at half maximum; e) using tetramethoxydiisindomethene-difluoroborate ( $\Phi = 0.51$ ) as reference.

**Figure 1.** Absorption (orange trace), emission (green trace) and excitation (dashed line) spectra of **3** in THF.



The absorption of the final compound **6** (Figure 2) shows three peaks. We can notice the presence of the structured peak around 320 nm due to the presence of thiophene fragments, overlapping with ( $S_0 \rightarrow S_2$ ) of the BODIPY.<sup>27</sup> The peak corresponding to the CT absorption band is now found at 537 nm and its  $\epsilon$  value is approximately twice as high as the one found for **3** ( $\epsilon$  about 50,000  $M^{-1}cm^{-1}$ ). The absorption spectrum also shows an intense peak ( $\epsilon$  around 90,000  $M^{-1}cm^{-1}$ ) at 737 nm corresponding to the  $\pi-\pi^*$  transition ( $S_0 \rightarrow S_1$ ) of the BODIPY unit in keeping with previous spectral analysis. The weak Stokes shift (715  $cm^{-1}$ ) and the short lifetime (around 1 ns) confirm that the excited state is likely a singlet with little reorganization in the excited state. The quantum yield is this time around 6 %. Once more, there was no influence of the solvent (THF, dichloromethane, toluene) on the fluorescence characteristics and the excitation spectrum matches fairly well the absorption spectrum in all cases. Notice that, relative to compound **5**, the non-radiative rate constant is larger than the radiative rate constant, a result in keeping with the energy gap law for dyes absorbing at low excitation energy.<sup>28</sup>

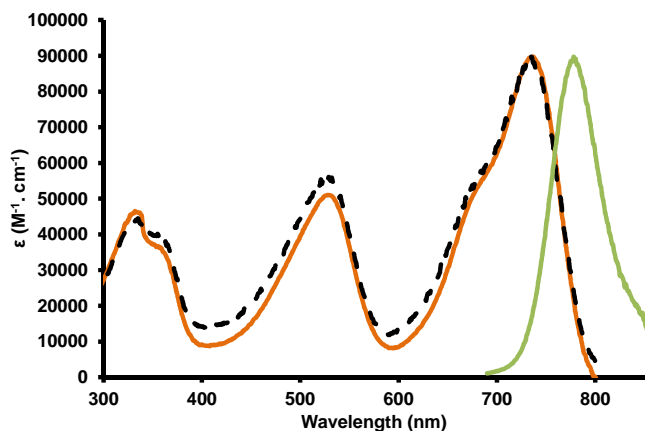


**Figure 2.** Absorption (orange trace), emission (green trace) and excitation (dashed line) spectra of **6** in THF.

The thin film absorption spectrum of **6** (Figure 3) shows a broad peak at 798 nm with a bathochromic shift of about 60 nm compared to the spectrum in solution and suggests the existence of strong  $\pi-\pi$  stacking interactions.<sup>29</sup> The low energy absorption edge leads to an optical band gap of 1.37 eV, which is low in comparison to most reported organic low band-gap materials and matches the optimal value predicted by Queisser et al<sup>30</sup> for homojunction solar cells.

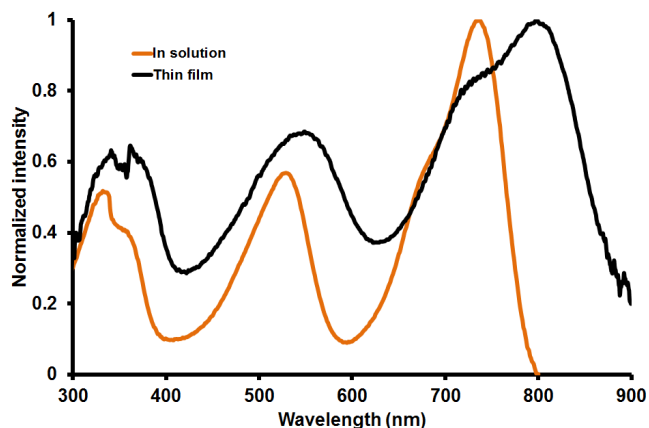


**Figure 3.** Absorption spectra of **6** in solution in THF (orange trace) and in thin film (black trace).

### 3.3. Redox properties

Cyclic voltammetry data obtained on **3**, **5**, and **6** in solution are shown in Figure 4. The spectrum of **5** shows only a reversible reduction at -0.79 V and no oxidation in the accessible redox window (up to 1.7 V), while the trimer **3** shows one reversible reduction at -1.37 V and one irreversible oxidation at +0.95 V. The voltammogram of **6** corresponds to a combination of both moieties: it shows three reversible reductions at -0.80 V, -1.32 V and -1.40 V and one irreversible oxidation at +0.71 V. From the splitting of the reduction wave at -1.37V we may infer that the two T-Bz-T side arms are not equivalent toward reduction processes. The HOMO level is estimated to -5.43 eV whereas the LUMO is around -4.08 eV. The electrochemical band-gap is thus equal to 1.35 eV, a value in keeping with the optical gap determined above (1.37 eV in Table 2).

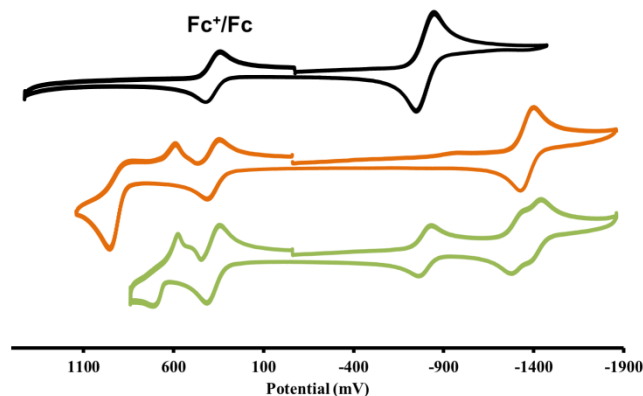


**Figure 4.** Cyclic voltammometry spectra of **5** (black trace), **3** (orange trace) and **6** (green trace).

**Table 2.** Experimentally determined energetic levels for compound **6**.

HOMO level	LUMO level	Electrochemical gap	Optical gap
-5.43 eV	-4.08 eV	1.35 eV	1.37 eV

### 3.4. DFT calculations

Density functional theory (DFT) calculations have been performed using SPARTAN 10 at the B3LYP/6-311+G\* level of theory in vacuum on dye **6** and are compared below to those obtained previously on another BODIPY dye named TB2 constructed with bis-thienylhexyl side arms (Figure 5).<sup>4</sup> Comparison with TB2 is motivated by: i) the similar molecular structure; ii) its high efficient in photon to electricity conversion in solar cells; iii) its ambipolar charge mobility in thin films.

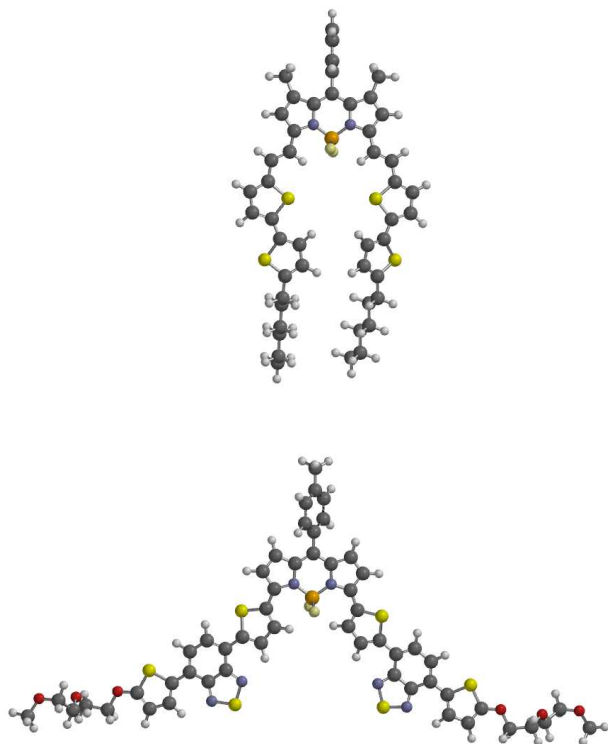


**Figure 5.** Conformation of dye TB2 (Top) and **6** (Bottom) and as calculated by DFT in vacuum.

The tolyl group is less twisted in the case of dye **6** ( $55^\circ$  for **6** and  $90^\circ$  for TB2) relative to the BODIPY core due to the absence of methyl groups in positions 1 and 7 of the BODIPY core. Both T-Bz-T segments (dye **6**) and T-T segments (TB2) show a high degree of planarity but are slightly more twisted relative to the BODIPY core for dye **6** ( $20^\circ$ ) than for TB2 ( $10^\circ$ ). This small twist angle difference is most likely due to the different links between the BODIPY core and the thiophene-based segments used for both dyes and has a negligible effect on the conjugation. The direct linking in compound **6** induces more steric crowing with the proton in the 2,6-positions relative to the double bond case (TB2) where the steric constraint is partially released. The most pronounced conformational difference between the two dyes is the orientation angle between the two thiophene-based segments that is as high as  $120^\circ$  for dye **6** while it is more than twice smaller for TB2. This difference is again mainly due to the single C-C bond between T-Bz-T and the BODIPY core (dye **6**). We expect that this

larger angle has a strong impact on the volume occupied by the dyes.

The calculated HOMO and LUMO orbitals are more delocalized for dye **6** than for TB2 (Figures 6 and 7). Even though the absolute values of the frontier energy levels obtained by DFT (given in the SI) may not be accurate, energy level shifts induced by changes in the molecular structure are more reliable. For dye **6** and TB2, the differences in frontier orbital energy levels are close to those found experimentally by cyclic voltammetry. The DFT LUMO level for dye **6** is found 0.3 eV above the one of TB2 while cyclic voltammetry gave LUMO values of -4.08 eV and -3.86 eV for dye **6** and TB2, respectively. Also, the DFT HOMO level for dye **6** is found 0.1 eV below that of TB2, which is again close to the measured values (-5.43 eV and -5.32 eV for dye **6** and TB2, respectively). In a previous study,<sup>4</sup> the LUMO level of TB2 and PC<sub>61</sub>BM were measured by cyclic voltammetry at -3.86 and -4.09 eV, respectively. Based on the present DFT calculations and cyclic voltammetry measurements, the energy offset between the LUMO level of dye **6** and the LUMO level of PC<sub>61</sub>BM may hinder exciton dissociation if **6** is to be used as electron donor material in donor/PC<sub>61</sub>BM blends. Yet, the relatively large span in reported PC<sub>61</sub>BM LUMO level values may reflect the influence of the degree of fullerene aggregation on the LUMO value, which varies with blend composition and processing conditions and is difficult to anticipate. Also, since a deep HOMO level is a prerequisite for air stable devices and a high open circuit voltage, it remains interesting to investigate the photovoltaic properties of **6**/PC<sub>61</sub>BM blends and to evaluate the impact of the exciton dissociation bottleneck as well as its potential for chemically stable high performance solar cells (see below).<sup>31</sup>

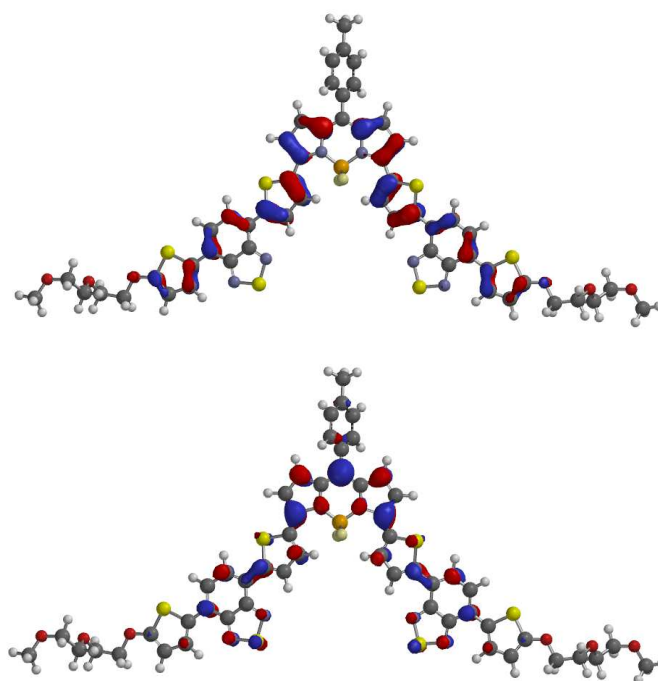




**Figure 6.** HOMO (Top) and LUMO (Bottom) orbitals for dye **6**. (top) and TB2 (bottom) as calculated by DFT in vacuum.

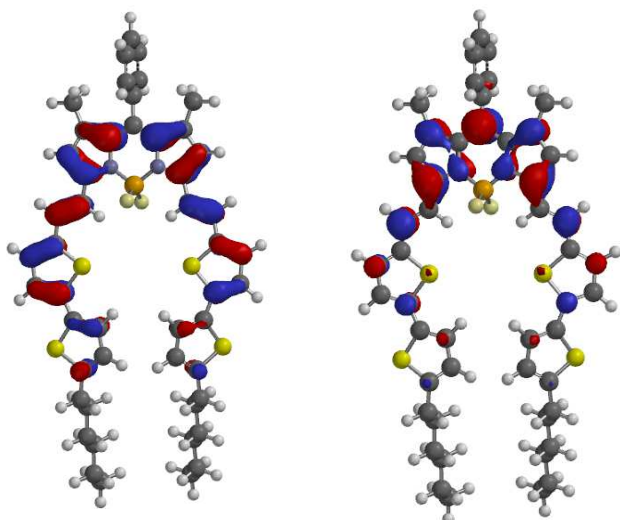


**Figure 7.** HOMO (Left) and LUMO (Right) orbitals for TB2 as calculated by DFT in vacuum.

### 3.5. AFM measurements

The morphology of the dye **6**/PCBM films was investigated by AFM. Two representative topography images of a film including a 1/2 ratio of dye **6**/PC<sub>71</sub>BM (see SI) before and after annealing show no clear morphology differences indicating that the thermal annealing step does not change deeply the microphase separation. It is worth noting the low roughness of the films (maximum height value around 1.4 nm), which does not change after thermal annealing confirms that the BODIPY derivative does not crystallize during the thermal annealing.

### 3.6. Mobility measurements

Charge transport is another important issue that needs to be addressed when designing new molecules for photovoltaic applications. We therefore used dye **6** as semiconducting layer in thin film transistors and extracted the field-effect charge carrier mobilities from the transfer characteristics in the saturation regime on pristine films (the device characteristics are given in the SI). Although field-effect transistors probe charge transport in very specific conditions (parallel to the dielectric interface and under high charge carrier densities), the results can give insight into the correlation between the molecular structure and charge transport properties.<sup>32</sup> In particular, the field-effect mobilities can be compared to those of TB2, which we take as a reference.

Interestingly, compound **6** exhibits a rather uncommon ambipolar nature with well-balanced hole and electron mobilities (Figure 8 and S2). This behavior is not surprising given the deep LUMO level of this dye and considering previous observations done on TB2, which presented ambipolar charge transport.<sup>4</sup> The electron and hole mobilities of **6** are in the lower range of  $10^{-4}$  cm<sup>2</sup> V<sup>-1</sup>.s<sup>-1</sup> which is significantly lower than those observed for TB2, but does not necessarily impede its utilization as donor material in a BHJ solar cell.

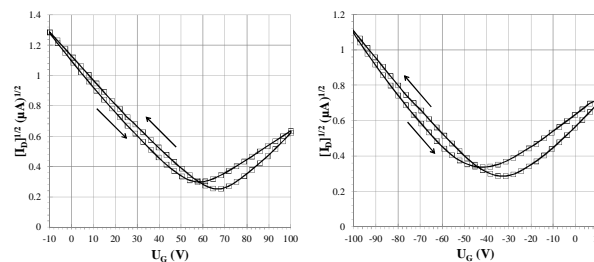


**Figure 8.** Transfer characteristics in saturation regime obtained for electrons (left) and holes (right) on a pristine film.  $I_D$  is the drain current and  $U_G$  is the gate voltage. The drain voltage was 100 V and -100 V for electrons and holes, respectively.

### 3.7. Photovoltaic devices elaboration and characterization

Bulk heterojunction devices were elaborated with a standard ITO/PEDOT:PSS/active layer/Al or Ca-Al structure. The active layer has been deposited by spin coating from organic solutions of compound **6** and PCBM derivatives. Several conditions, including different solvents, different concentrations, the use of two different PCBM derivatives (either PC<sub>61</sub>BM or PC<sub>71</sub>BM) and variations in the donor/acceptor weight ratio, have been tested. Some representative device properties are summarized in Table 3 (more details about the experimental conditions can be found in the Supporting Information). Typical current-voltage curves are displayed in Figure 9. Surprisingly, the elaboration process has only a minor impact on the measured power conversion efficiency (PCE), which remains close to 1.2 % independently of the solvent nature and of the fullerene derivatives used. The major performance limiting factors are a low fill factor (close to 33%) and rather low short-circuit current density. The latter is much below expectation if we consider the rather broad absorption band and high extinction coefficient of **6**. The fill factor in turn is linked to the low parallel resistance ( $R_{shunt}$ ) measured under illumination (inverse slope at short-circuit current). Increasing the active layer thickness by using more concentrated solutions to enhance light absorption did lead only to a weak increase in device performances (similar fill factors but slightly higher short-circuit currents were obtained) (see Table S2).

The low FF (or low parallel resistance) could originate from either fast charge carrier recombination (geminate or non-geminate) or field-assisted exciton dissociation. In the former case, increasing the electric field by reverse biasing the device would lower the sweep-out time, minimize the loss of charge carriers by recombination and give rise to higher photocurrents (defined as the difference between light and dark current at a given voltage). The weak thickness dependence of the fill factor and shunt resistance points out that charge extraction may not be the major bottleneck, despite the relatively low charge carrier mobilities. This conclusion is also inline with the weak offset between the LUMO levels of dye **6** and PCBM, which suggests the current D/A interface energetics to be unfavorable to exciton dissociation. On the other hand, the open-circuit voltage  $V_{oc}$  varies between 0.6 and 0.7 V, which is well below the value expected according to the frequently observed linear

dependence of  $V_{oc}$  on the difference between the acceptor LUMO and the donor HOMO level in BHJ devices (Assuming a PCBM LUMO level of  $-4$  eV and an energy loss  $\Delta E$  due to recombination of  $\sim 0.3$  V, leads to a value well above 1V).<sup>29</sup> High recombination rates or poor charge generation are possible reasons for this discrepancy. Distinguishing between both processes mentioned above is not trivial and requires utilization of advanced time-resolved measurements. These however lie beyond the scope of the present article.

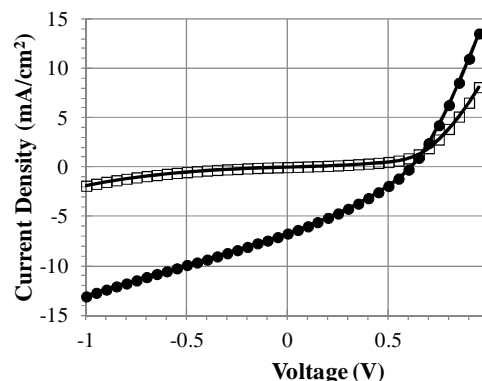


**Figure 9.** Current density versus voltage in the dark (open symbols) and under standard AM1.5G ( $100 \text{ mW/cm}^2$ ) illumination (closed symbols) for the last conditions of Table 3.

**Table 3.** Selected thin-films compositions and deposition conditions with associated OPV performances

Acceptor	Ratio (6/PCBM)	BODIPY dye concentration	Solvent	Cathode	$V_{oc}$ (V)	$J_{sc}$ ( $\text{mA/cm}^2$ )	FF	PCE (%)	$R_{shunt}$ ( $\Omega$ )
PC <sub>61</sub> BM	1/1.5	5 mg/mL	CHCl <sub>3</sub>	Al	0.69	5.2	0.32	1.15	1700
PC <sub>61</sub> BM	1/2	3 mg/mL	CHCl <sub>3</sub>	Ca/Al	0.62	5.8	0.35	1.26 <sup>b)</sup>	1550
PC <sub>71</sub> BM	1/2	10 mg/mL	CB+0.3 vol % DIO <sup>a)</sup>	Al	0.61	7.4	0.28	1.26 <sup>c)</sup>	1250

a) CB denotes for chlorobenzene and DIO denotes for 1,8-diiodooctane

b) Annealed for 10 minutes at  $60^\circ\text{C}$  prior to cathode deposition

c) Annealed for 10 minutes at  $80^\circ\text{C}$  and at  $100^\circ\text{C}$  for 3 minutes.

### 3.8. Comparison with related BODIPY based devices.

**Table 4.** Selected OPV data for analogous BODIPY-based molecules and polymers depicted in Figure 10.

Cmpd	Device	$J_{sc}$ ( $\text{mA}\cdot\text{cm}^{-2}$ )	$V_{oc}$ (V)	FF	$\eta$ (%)	$\mu_h$ ( $\text{V}\cdot\text{cm}^{-2}\cdot\text{s}^{-1}$ )	$\mu_e$ ( $\text{V}\cdot\text{cm}^{-2}\cdot\text{s}^{-1}$ )
<b>6</b>	ITO/PEDOT:PSS/6:PC <sub>61</sub> BM/Ca/Al	5.8	0.62	0.35	1.26	$\sim 10^{-4}$ a)	$\sim 10^{-4}$ a)
<b>TB2</b> <sup>d)</sup>	ITO/PEDOT:PSS/TB2:PC <sub>61</sub> BM/Ca/Al	14.3	0.70	0.47	4.7	$\sim 10^{-3}$ a)	$\sim 10^{-3}$ a)
<b>A</b> <sup>33</sup>	ITO/Ca/A:PC <sub>71</sub> BM/MoO <sub>3</sub> /Ag	8.3	0.99	0.40	3.22	$4.1 \times 10^{-6}$ b)	$2.3 \times 10^{-4}$ b)
<b>B</b> <sup>33</sup>	ITO/Ca/B:PC <sub>71</sub> BM/MoO <sub>3</sub> /Ag	7.5	0.93	0.37	2.56	$1.2 \times 10^{-6}$ b)	$6.0 \times 10^{-5}$ b)
<b>C</b> <sup>34</sup>	ITO/PEDOT:PSS/C:PC <sub>61</sub> BM/Al	6.9	0.74	0.38	2.17	$9.7 \times 10^{-5}$	-
<b>D</b> <sup>35</sup>	ITO/PEDOT:PSS/D:PC <sub>61</sub> BM/Al	4.8	0.80	0.51	2.0	$3.0 \times 10^{-7}$	-
<b>E</b> <sup>36</sup>	ITO/PEDOT:PSS/E:PC <sub>61</sub> BM/Ca/Al	2.65	0.88	0.26	0.62	-	-
<b>F</b> <sup>37</sup>	ITO/PEDOT:PSS/F:PC <sub>71</sub> BM/Al	7.87	0.31	0.39	0.95	$1.5 \times 10^{-5}$ c)	$7.7 \times 10^{-5}$ c)

<sup>a</sup> Values obtained by OFET measurements on pure materials, <sup>b</sup> Values obtained by SCLC measurements on blends with PC<sub>71</sub>BM, <sup>c</sup> Values obtained by TOF measurements on pure materials.

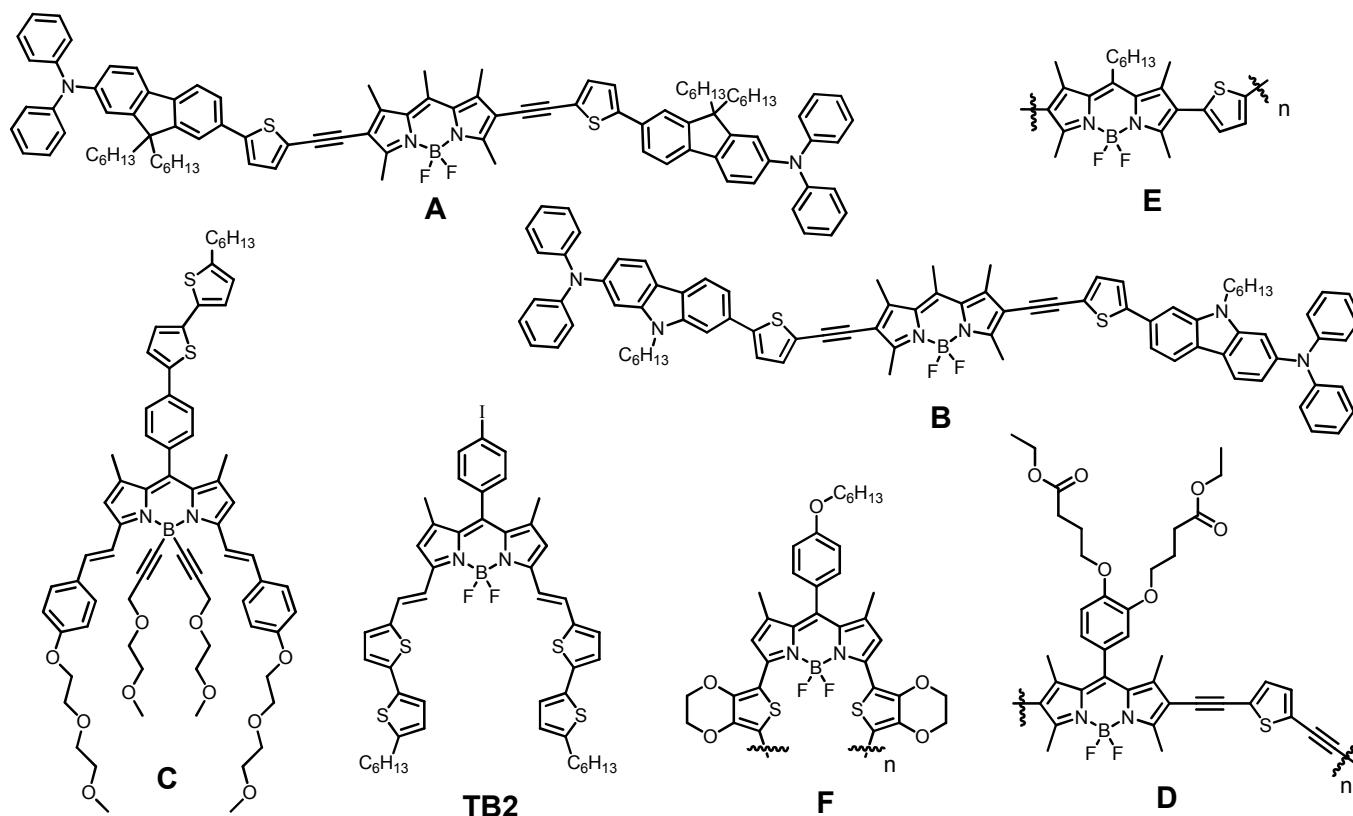


**Figure 10.** Chemical structures of related BODIPY frameworks studies in bulk heterojunction solar cells.

By comparison of BODIPY based small molecules and polymeric materials it appears that ambipolar charge transport has been observed in both categories and the lead is held by **TB2** which also display the highest photon to current conversion. This behaviour is surely due to the deep LUMO level usually measured in BODIPY based materials. However, a further comparison on the basis of values found in literature (and reported in the above table) is hazardous as they are provided by different techniques, including space charge limited current (SCLC) on blends, time of flight (TOF) or OFET on pure materials. In most cases the short-circuit current ( $J_{SC}$ ) is rather high reaching 14.3 mA/cm<sup>2</sup> in the best case but the fill factor ( $FF$ ) remains modest (Table 4). Further comparison between those materials must be taken with care because the structures of devices (standard versus inverted cells), the metallic electrodes, the interfacial layers and the device active areas are significantly different.

#### 4. Conclusion

We have synthesized a new deep-purple-grey 4,4-difluoro-4-bora-3a,4a-diaza-s-indacene dye (BODIPY) incorporating two thiophene-benzothiadiazole-thiophene units bridging an unsubstituted BODIPY core at the wings. In the electronic absorption spectra, an effective charge transfer band appears at 537 nm relative to 479 nm in the thiophene-benzothiadiazole-thiophene module due to interaction between the strong “push” thiophene units at the periphery and the central

benzothiadiazole “pull” unit. This is an interesting approach, which also contributes to the increase of photon absorption either in solution or in the thin film. This strong absorption and redox activity of this dye enable the preparation of bulk heterojunction with thin films blended with [6,6]phenylC<sub>61</sub>or71butyricacidmethylester PC<sub>n</sub>BM (n = 61 or 71). Promising efficiencies around 1.25% were obtained, these reproducible efficiencies are weakly depending on the composition, thickness of the films and nature of the electrodes. The synthetic routes outlined here provide the scope to further tune the performance of the solar cells by post-functionalization of the 2,6 or (β,β’-pyrrolic positions) with electron donating modules suitable to increase the driving force for photoinduced electron injection in the PCBM acceptor.

#### Acknowledgements

We thank the Centre National de la Recherche Scientifique (CNRS), the Engineering School of Chemistry (ECPM) and Rhin-Solar supported by the European Fund for Regional Development (FEDER) in the framework of the Programme INTERREG IV Upper Rhine, Project nr C25 for financial support of this work. N. Zimmermann from ICube in Strasbourg is kindly acknowledged for his help in the photovoltaic device elaboration.

#### Notes and references

<sup>a</sup> Institut de Chimie et Procédés pour l’Energie, l’Environnement et la Santé (ICPEES), Laboratoire de Chimie Moléculaire et Spectroscopies Avancées LCOSA, Ecole Européenne de Chimie, Polymères et

Matériaux, ICPEES-LCOSA, UMR 7515 associé au CNRS, 25 rue Becquerel, 67087 Strasbourg Cedex 02, France, E-mail: ziessel@unistra.fr

<sup>b</sup> Institut de Chimie et Procédés pour l'Energie, l'Environnement et la Santé (ICPEES), Université de Strasbourg, Ecole Européenne de Chimie, Polymères et Matériaux, 25 rue Becquerel, 67087 Strasbourg, France,

<sup>c</sup> Laboratoire ICube, Université de Strasbourg, CNRS, 23 rue du Loess, 67037 Strasbourg, France

## References

- <sup>1</sup> T. M. Figueira-Duarte and K. Müllen, *Chem. Rev.*, 2011, **111**, 7260.
- <sup>2</sup> (a) G. Yu, J. Gao, J. C. Hummelen, F. Wudl and A. J. Heeger, *Science*, 1995, **270**, 1789. (b) T. S. van der Poll, J. A. Love, T.-Q. Nguyen and G. C. Bazan, *Adv. Mater.*, 2012, **24**, 3646; (c) Y. Sun, G. C. Welch, W. L. Leong, C. J. Takacs, G. C. Bazan and A. J. Heeger, *Nat. Mater.*, 2012, **11**, 44; (d) Z. Li, G. He, X. Wan, Y. Liu, J. Zhou, G. Long, Y. Zuo, M. Zhang and Y. Chen, *Adv. Energy Mater.*, 2012, **2**, 74; (e) J. Y. Zhou, X. J. Wan, Y. S. Liu, Y. Zuo, Z. Li, G. R. He, G. K. Long, W. Ni, C. X. Li, X. C. Su and Y. S. Chen, *J. Am. Chem. Soc.*, 2012, **134**, 16345.
- <sup>3</sup> (a) G. Ulrich, R. Ziessel and A. Harriman, *Angew. Chem. Int. Ed.*, 2008, **47**, 1184-1201. (b) A. Loudet and K. Burgess, *Chem. Rev.*, 2007, **107**, 4891-4932. (c) R. Ziessel, G. Ulrich and A. Harriman, *New J. Chem.*, 2007, **31**, 496-501.
- <sup>4</sup> T. Bura, N. Leclerc, S. Fall, P. Lévêque, T. Heiser, P. Retailleau, S. Rihn, A. Mirloup and Ziessel, *R. J. Am. Chem. Soc.* **2012**, *134*, 17404-17407.
- <sup>5</sup> R. Fitzner, E. Reinold, A. Mishra, H. Mena-Osteritz, Zielke, C. Körner, K. Leo, M. Riede, M. Weil, O. Tsaryova, A. Weiss, C. Uhrich, M. Pfeiffer and P. Bäuerle, *Adv. Funct. Mater.* 2011, **21**, 897-910.
- <sup>6</sup> (a) B. Walker, A. B. Tamayo, X.-D. Dang, P. Zalar, J. H. Seo, A. Garcia, M. Tantiwivat and T.-Q. Nguyen, *Adv. Funct. Mater.* 2009, **19**, 3063-3069. (b) T. Bura, N. Leclerc, R. Bechara, P. Lévêque, T. Heiser and R. Ziessel, *Adv. Energy Mater.*, 2013, **3**, 1118-1124.
- <sup>7</sup> (a) G. Wei, S. Wang, K. Sun, M. E. Thompson and S. R. Forrest, *Adv. Eng. Mater.* 2011, **2**, 184-187. (b) A. Ajayaghosh, *Acc. Chem. Res.* 2005, **38**, 449-459.
- <sup>8</sup> W. W. H. Wong, T. B. Singh, D. Vak, W. Pisula, C. Yan, X. Feng, E. L. Williams, K. L. Chan, Q. Mao, D. J. Jones, C.-Q. Ma, K. Müllen, P. Bäuerle and A. B. Holmes *Adv. Funct. Mater.* 2010, **20**, 927-938.
- <sup>9</sup> N. M. Kronenberg, M. Deppisch, F. Würthner, H. W. A. Ladermann, K. Deing and K. Meerholz, *Chem. Commun.* 2008, 6489-6491.
- <sup>10</sup> H. Bürckstümmer, E. V. Tulyakova, M. Deppisch, M. R. Lenze, N. M. Kronenberg, M. Gsänger, M. Stolte, K. Meerholz and F. Würthner, *Angew. Chem. Int. Ed.* 2011, **4506**, 11628-11632.
- <sup>11</sup> Y. Sun, G. C. Welch, W. L. Leong, C. J. Takacs, G. C. Bazan and A. J. Heeger, *Nature Mater.* 2011, **11**, 44-48.
- <sup>12</sup> R. Ziessel, *Comptes Rendus Chim.* 2007, **10**, 622-629.
- <sup>13</sup> (a) T. Rousseau, A. Cravino, T. Bura, G. Ulrich, R. Ziessel and J. Roncali, *Chem. Commun.* 2009, 1673-1675. (b) T. Bura, N. Leclerc, S. Fall, P. Lévêque, T. Heiser and R. Ziessel, *Org. Lett.*, 2011, **22**, 6030-6033.
- <sup>14</sup> A. Sutter, P. Retailleau, W.-C. Huang, H.-W. Lin, and R. Ziessel, *New J. Chem.*, 2014, **38**, 1701-1710.
- <sup>15</sup> (a) S. Erten-Ela, M. D. Yilmaz, B. Icli, Y. Dede, S. Icli and E. U. Akkaya, *Org. Lett.*, 2008, **10**, 3299-3302. (b) S. Kolemen, Y. Cakmak, S. Erten-Ela, Y. Altay, J. Brendel, M. Thelakkat and E. U. Akkaya, *Org. Lett.* 2010, **12**, 3812-3815. (c) S. Kolemen, O. A. Bozdemir, Y. Cakmak, G. Barin, S. Erten-Ela, M. Marszalek, J.-H. Yum, S. M. Zakeeruddin, M. K. Nazeeruddin, M. Grätzel, and E. U. Akkaya, *Chem. Sci.* 2011, **2**, 949-954.
- <sup>16</sup> D. Kumaresan, R. P. Thummel, T. Bura, G. Ulrich and R. Ziessel *Chem. Eur. J.* 2009, **15**, 6335-6339.
- <sup>17</sup> C. Qin , A. Mirloup , N. Leclerc , A. Islam , A. El-Shafei , L. Han , and R. Ziessel, *Adv. Energy Mater.* 2014, DOI: 10.1002/aenm.201400085.
- <sup>18</sup> I. Culloch, M. Heeney, C. Bailey, K. Genevicius, I. MacDonald, M. Shkunov, D. Sparrowe, S. Tierney, R. Wagner, W. Zhang, M. L. Chabiny, R. J. Kline, M. D. McGehee, M. F. Toney, *Nat. Mater.* 2006, **5**, 328.
- <sup>19</sup> J. Liu, R. Zhang, G. Sauvé, T. Kowalewski and R. D. McCullough, *J. Am. Chem. Soc.*, 2008, **130**, 13167.
- <sup>20</sup> I. Saka, R. Zhang, J. Liu, D.-M. Smilgies, T. Kowalewski and R. D. McCullough, *Chem. Mater.*, 2010, **22**, 4191.
- <sup>21</sup> Zhou, J.; Wan, X.; Liu, Y.; Long, G.; Wang, F.; Li, Z.; Zuo, Y.; Li, C.; Chen, Y., *Chem. Mater.*, 2011, **23**, 4666-4668.
- <sup>22</sup> Liu, Y.; Wan, X.; Wang, F.; Zhou, J.; Long, G.; Tian, J.; Chen, Y. *Adv. Mater.*, 2011, **23**, 5387-5391.
- <sup>23</sup> (a) M. Zhang, H. N. Tsao, W. Pisula, C. Yang, A. K. Mishra and K. Mullen, *J. Am. Chem. Soc.*, 2007, **129**, 3472-3473. (b) H. N. Tsao, D. M. Cho, I. Park, M. R. Hansen, A. Mavrinskiy, D. Y. Yoon, R. Graf, W. Pisula, H. W. Spiess and Müllen, K., *J. Am. Chem. Soc.* 2011, **133**, 2605- 2612. (c) Z. Zhu, D. Waller, R. Gaudiana, M. Morana, D. Mühlbacher, M. Scharber and C. Brabec, *Macromolecules* 2007, **40**, 1981- 1986. (d) P. M. Beaujuge, H. N. Tsao, M. R. Hansen, C. M. Amb, C. Risko, J. Subbiah, K. R. Choudhury, A. Mavrinskiy, W. Pisula, J.-L. Bredas, F. So, K. Müllen and J. R. Reynolds, *J. Am. Chem. Soc.*, 2012, **134**, 8944-8957. (e) R. C. Coffin, J. Peet, J. Rogers and G. C. Bazan, *Nature Chem.*, 2009, **1**, 657-661. (f) S. H. Park, A.

- Roy, S. Beaupre, S. Cho, N. Coates, J. S. Moon, D. Moses, M. Leclerc, K. Lee and A. J. Heeger, *Nat. Photonics*, 2009, **3**, 297-303.
- <sup>24</sup> X. Guo, N. Zhou, S. J. Lou, J. W. Hennek, R. P. Ortiz, M. R. Butler, P.-L. T. Boudreault, J. Strzalka, P.-O. Morin, M. Lecherc, J. T. Lopez Navarrete, M. A. Ratner, L. X. Chen, R. P. H. Chang, A. Facchetti and T. J. Marks, *J. Am. Chem. Soc.*, 2012, **134**, 18427-18439.
- <sup>25</sup> Y. Zhou, Q. He, Y. Yang, H. Zhong, C. He, G. Sang, W. Liu C. Yang, F. Bai and Y. Li, *Adv. Funct. Mater.*, 2008, **18**, 3299-3306.
- <sup>26</sup> M. Rajeswara Rao, Shaikh M. Mobin and M. Ravikanth *Tetrahedron*, **2010**, 66, 9, 1728-1734.
- <sup>27</sup> A. Burghart, H. J. Kim, M. B. Welch, L. H. Thorensen, J. Reibenspies, K. Burgess, F. Bergstrom and L. B. A. Johansson, *J. Org. Chem.* **1999**, 64, 7813-7819.
- <sup>28</sup> M. Bixon, J. Jortner, J. Cortes, H. Heitele and M. E. Michel-Beyerle *J. Phys. Chem.* 1994, **98**, 7289-7299.
- <sup>29</sup> J. Mizuguchi and G. Wooden *Ber. Bunsen. Phys. Chem.* 1991, **95**, 1264-1274 and references cited therein.
- <sup>30</sup> W. Shockley and H.J. Queisser, *J. Appl. Phys.* 1961, **32**, 510-519.
- <sup>31</sup> G. Dennler, M. C. Scharber and C. J. Brabec, *Adv. Mater.* 2009, **21**, 1323-1338.
- <sup>32</sup> S. Fall, L. Biniek, N. Leclerc, P. L  v  que and T. Heiser, *Appl. Phys. Lett.* 2012, **101**, 123301-123303.
- <sup>33</sup> H.-Y. Lin, W.-C. Huang, Y.-C. Chen, H.-H. Chou, C.-Y. Hsu, J. T. Lin and H.-W. Lin, *Chem. Commun.* 2012, **48**, 8913-8915.
- <sup>34</sup> T. Rousseau, A. Cravino, E. Ripaud, P. Leriche, S. Rihn, A. De Nicola, R. Ziessel and J. Roncali, *Chem. Commun.* 2010, **46**, 5082-5084.
- <sup>35</sup> B. Kim, Ma, B. V. R. Donuru, H. Liu and J. M. Fr  chet, *J. Chem. Commun.* 2010, **46**, 4148-4150.
- <sup>36</sup> D. Cortizo-Lacalle, C. T. Howells, S. Gambino, F. Vilela, Z. Vobecka, N. J. Findlay, A. R. Inigo, S. A. J. Thomson, P. J. Skabara and I. D. W. Samuel, *J. Mater. Chem.* 2012, **22**, 14119-14126.
- <sup>37</sup> S. P. Economopoulos, C. L. Chochos, H. A. Ioannidou, M. Neophytou, C. Charilaou, G. A. Zissimou, J. M. Frost, T. Sachetan, Shahid, J. Nelson, M. Heeney, D. D. C. Bradley, G. Itskos, P. A. Koutentis and M., S. A. Choulis *R.C.S. Advances* 2013, **3**, 10221-10229.